J. Appl. Comput. Mech., 8(4) (2022) 1222-1235
DOI: 10.22055/JACM.2021.38569.3248

ISSN: 2383-4536
jacm.scu.ac.ir

Shahid Chamran University of Ahvaz

Journal of Applied and Computational Mechanics

Research Paper

Pull-in Phenomenon in the Electrostatically Micro-switch Suspended between Two Conductive Plates using the Artificial Neural Network

Mortaza Aliasghary[1], Hamed Mobki[2], Hassen M. OUAKAD[3]

[1] Electrical Engineering Department, Faculty of Industrial Technologies, Urmia University of Technology (UUT), Urmia, Postal Code: 57166-17165 Iran, Email: m.aliasghary@uut.ac.ir
[2] Department of Engineering, German University of Technology in Oman, Athaibah, Muscat, Postal Code: 1816, Oman, Email: hamedmobki@live.com
[3] Mechanical and Industrial Engineering Department, Sultan Qaboos University, Al Khoudh, Muscat, Postal Code:123, Oman, Email: houakad@squ.edu.om

Received September 14 2021; Revised November 04 2021; Accepted for publication November 11 2021.
Corresponding author: H. Mobki (hamedmobki@live.com)

Abstract. Artificial Neural Networks (ANN) are designed to evaluate the pull-in voltage of MEMS switches. The mathematical model of a micro-switch subjected to electrostatic force is preliminarily illustrated to get the relevant equations providing static deflection and pull-in voltage. Adopting the Step-by-Step Linearization Method together with a Galerkin-based reduced order model, numerical results in terms of pull-in voltage are obtained to be employed in the training process of ANN. Then, feed forward back propagation ANNs are designed and a learning process based on the Levenberg-Marquardt method is performed. The ability of designed neural networks to determine pull-in voltage have been compared with previous results presented in experimental and theoretical studies and it has been shown that the presented method has a good ability to approximate the threshold voltage of micro switch. Furthermore, the geometric and physical effect of the micro-switch on the pull-in voltage was also examined using these designed networks and relevant findings were provided.

Keywords: MEMS; Pull-in Instability; Electrostatic; Artificial Neural Network.

1. Introduction

Micro-Electro-mechanical systems (MEMS) have recently attracted the attention of many researchers and industries. This was partially attributed to such major structures as high performance [1], order of magnitude [2], electrically controlled [3, 4], fast response [5], possibility for batch fabrication [6], compatibility with CMOS fabrication [7], and very low energy consumption [8].

Most of the MEMS structures rely on the electrostatic actuation for their operation, due to the simplicity of the excitation mechanism, the requirement for only few mechanical components, as well as small voltage levels for proper actuation [9, 10]. Other MEMS structures' excitations include piezoelectric [11], pneumatic [12], electromagnetic [13], and thermal excitation [14]. Typically, in such structures, a beam or plate is suspended over a fixed surface or between two fixed surfaces. When an electrostatic voltage is applied to a moving part, its elastic stiffness decreases, and at a specific voltage known as pull-in voltage, the stiffness is lost and becomes unstable, with the moving part being affected by sudden and unpredictable displacements [9]. The pull-in instability is one of the most important phenomena usually observed in the majority of MEMS/NEMS structures and numerous studies have been conducted in this area using different numerical approaches [15-20]. Correspondingly, experimental analysis of determining the pull-in instability of MEMS structures were investigated and published in several references [21-24]. Jianxin Han et al. [25] studied the pull-in instability of MEMS actuators via a generalized one-degree-of-freedom discretized using the differential quadrature method and then compared the results with a COMSOL Finite-Elements (FE) 2D model. Same instability for different MEMS structures were investigated based on FE method and using IntelliSuite software in numerous references [26-31]. Recently, significant studies have been conducted on the instability analysis of MEMS/NEMS structures by considering stress-driven nonlocal integral models and couple stress theory [32-42]. For such modeling, the instability voltage can also be determined using the Artificial Neural Network. The abovementioned experimental and numerical investigations suggested that determining the pull-in voltage is a time-consuming process.

To this end, this work is considering designing Artificial Neural Networks schemes to determine the pull-in voltage of micro-switches and actuators. The pull-in voltage is first to be determined for several samples assuming various physical and geometric specifications using the method provided in reference [43]. Then, to train the ANNs, the physical and geometric specifications of the structure are considered as the inputs to these networks. Training of the ANNs is performed assuming two and three layers of different neurons. The accuracy of the designed neural network, the pull-in voltage of the micro-structures, whose pull-in states had been provided in previous studies, will be examined. Generally, novelty of this work deals with the application of Artificial

Published online: November 16 2021

Neural Networks to obtain the pull-in voltage of electro-statically actuated micro-beam suspended between two stationary conducted plates [43]. Thus, an in-depth illustration of the adopted ANNs design is supposed to be provided to increase the value of the present work [43].

This study is organized as: In the next section studied micro switch is introduced and its geometric and physical features will be presented. Section 3 overviews the theoretical modeling used to obtain of static deflection and pull-in voltage of the micro switch subjected to electrostatic force. Section 4 deals with design of artificial neural networks to estimate of pull-in voltage and presenting relevant results. Finally, Section 5 presents the concluding remarks of this paper.

2. Micro-switch Design

"Figure 1a." shows the 2D schematic view of the assumed micro-switch in which a beam with length L, is suspended between two stationary conductor plates. The relevant gaps between beam and stationary bottom and upper plates are both considered the same and equal to G_1. The shown beam is to move toward lower or upper plates by applying DC voltages of V_1 and V_2, respectively. The bending condition of beam in attraction towards the plates depends on magnitude of applied voltages. If $V_1 > V_2$ beam bends towards the lower plate and for $V_1 < V_2$ beam gets closer to upper plate. But for $V_1 = V_2$, beam settles in its primary positions until reaching pull-in voltage. Schematic view of actuated MEM switch for the condition of $V_1 > V_2$ is depicted in "Fig. 1c." As shown in this figure the beam bends toward lower plate and its maximum deflection occurs in the middle with $x = L/2$. Also, bending view of micro beam for $V_1 < V_2$ can be observed in "Fig. 1d." Furthermore, cross section area of micro-switch is depicted in "Fig. 1-b.". As can be seen from this schematic, its width and thickness are respectively equal with b and h and the moving beam is assumed to be made from an isotropic material with modulus of elasticity *E*, cross section area of *A* and moment of inertia *I*.

3. Mathematical Modeling

3.1. Micro-beam static deflection governing differential equation

In this section the main formulation for extracting the micro-beam, "Fig. 1a.", static deflections as well as its respective pull-in voltage are presented. The governing equation of the static deflection of micro-beam will be first presented. Then, the numerical approach to solve for the obtained governing equation and then acquire the static pull-in voltage will be presented. The static deflection governing equation of the micro-switch of "Fig. 1a." is obtained assuming a linear Euler Bernoulli beam theory and can be written as follows [43]:

$$EI\frac{\partial^4\hat{w}}{\partial\hat{x}^4}=\frac{b\varepsilon_0}{2}\left(\frac{V_1^2}{(G_1-\hat{w})^2}-\frac{V_2^2}{(G_1+\hat{w})^2}\right) \tag{1}$$

where $\hat{w}(x)$ represents the flexural deflection of the micro-beam with respect to the lower plate and $\varepsilon_0=8.854\times10^{-12}C^2N^{-1}m^{-2}$ is the permittivity of vacuum. The right-hand side terms of "Eq. (1)" show the resultant electrostatic forces from lower and upper plates, respectively, per unit length ($q_{elec}(V_1,V_2,\hat{w})$).

For convenience "Eq. (1)" can be rewritten in a non-dimensional form while exploiting the following non-dimensional parameters:

$$w=\frac{\hat{w}}{G_1}\quad,\quad y=\frac{\hat{y}}{G_1}\quad,\quad x=\frac{\hat{x}}{L}\quad,\quad p=\frac{V_2}{V_1} \tag{2}$$

Therefore, considering these normalizing parameters, "Eq. (1)" can be re-written as follows:

$$\frac{\partial^4 w}{\partial x^4}=\alpha V_1^2\left[\frac{1}{(1-w)^2}-\frac{p^2}{(s+w)^2}\right] \tag{3}$$

where α is the dimensionless parameter of the electrostatic force and equals with $\alpha=\varepsilon_0 bL^4/2EIG_1^3$.

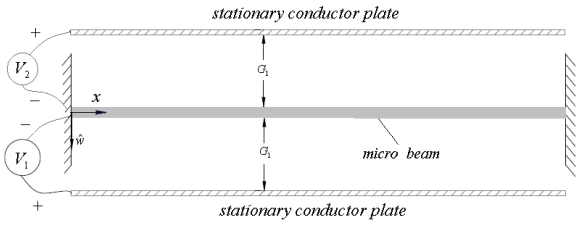

a. A beam-based MEM switch

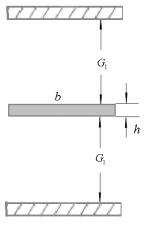

b. Cross section of the micro beam

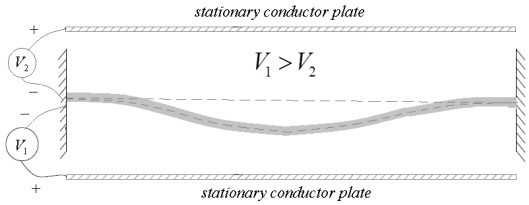

c. schematic view of actuated MEM switch for the condition of $V_1 > V_2$

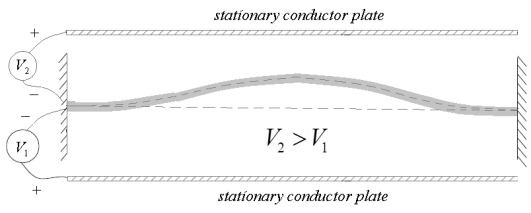

d. schematic view of actuated MEM switch for the condition of $V_2 > V_1$

Fig. 1. Schematic view of a beam-based MEM switch.

3.2. Numerical Approach

As “Eq. (3)” contains nonlinear terms, the analytical solution methods may not be applicable to obtain the pull-in voltage ‘ $V_{pull\text{-}in}$ ’. Therefore, a Step-by-Step Linearization Method (SSLM) [43] together with a Galerkin-based reduced order mode (ROM) are employed to find the micro-beam static deflection as well its respective pull-in voltage. The use of the static SSLM method is mainly based upon gradually and smoothly introducing the nonlinear electrostatic forces governed by the applied voltages V_1 and V_2 . These voltages are to be increased from zero to higher values assuming a smooth step-by-step process while satisfying the quasi-equilibrium condition. It is worth nothing that, the final reached value indicates the pull-in voltage. For implementing this method, the superscript ‘i’ refers to the iteration on the DC voltage step and w^i represents the non-dimensional displacement of the micro-beam, subjected to both V_1^i and V_2^i . By increasing the applied DC voltages V_1^i and V_2^i , the dimensionless deflection at (i+1)th step can be obtained as follows:

$$V_1^{i+1} = V_1^i + \delta V_1 \quad \& \quad V_2^{i+1} = V_2^i + \delta V_2 \quad \Rightarrow \quad w^{i+1} = w^i + \delta w \tag{4}$$

Through applying an infinitesimal values for both δV_1 and δV_2 , the δw will be small enough that the Taylor series expansion can be assumed in each step instead of exact main excitation function. The equation for the ith and (i+1)th steps can both be written respectively as follows:

$$\frac{d^4 w^i}{dx^4} = q_{elect}\left(V_1^i, V_2^i, w^i\right) \tag{5}$$

$$\frac{d^4 w^{i+1}}{dx^4} = q_{elect}\left(V_1^{i+1}, V_2^{i+1}, w^{i+1}\right) \tag{6}$$

Substituting w^{i+1} , V_1^{i+1} and V_2^{i+1} in “Eq. (6)” and implementing a Taylor series expansion, the resultant equation can be written in the following form:

$$\frac{d^4 w^i}{dx^4} + \frac{d^4(\delta w)}{dx^4} = q_{elec}(V_1^i, V_2^i, w^i) + \left(\frac{\partial q_{elec}}{\partial w}\Big|_{w^i}\right)\delta w + \frac{\partial q_{elec}}{\partial V_1}\delta V_1 + \frac{\partial q_{elec}}{\partial V_2}\delta V_2 \tag{7}$$

Subtracting “Eq. (5)” from “Eq. (6)” the required form for obtaining δw can be shown as:

$$\frac{d^4(\delta w)}{dx^4} - \left(\frac{\partial q_{elec}}{\partial w}\Big|_{w^i}\right)\delta w = + \frac{\partial q_{elec}}{\partial V_1}\delta V_1 + \frac{\partial q_{elec}}{\partial V_2}\delta V_2 \tag{8}$$

This above is a linear ordinary differential equation and can be solved using a Galerkin-based reduced-order method [43] where δw can be expressed as:

$$\delta w = \sum_{j=1}^{\infty} q_j \psi_j(x) \tag{9}$$

where $\psi_j(x)$ symbolizes the jth shape function which satisfies the boundary conditions of the micro-beam and for the fixed-fixed micro-beam is presented as [44]:

$$\psi_j(x) = \left(\cos\beta_j x - \cosh\beta_j x\right) - \frac{\cos\beta_j - \cosh\beta_j}{\sin\beta_j - \sinh\beta_j}\left(\sin\beta_j x - \sinh\beta_j x\right) \tag{10}$$

where for $j = 1:4$, $\beta_j = 4.7300$, 7.8532 , 10.9956 , 14.1372 .

The unknown δw is approximated by truncating the summation series to finite number, N as follows:

$$\delta w_N \cong \sum_{j=1}^{N} q_j \psi_j(x) \tag{11}$$

By substituting “Eq. (11)” into “Eq. (8)” and multiplying the outcome equation by $\psi_r(x)$ as a weight function, and integrating the outcomes from $x = 0$ to 1 , a set of algebraic equations will be extracted. Solving these set of equations, the deflection at any given point under applied voltage and the pull-in voltage of the micro-beam can be obtained.

4. Artificial Neural Network for the Pull-in Voltage Estimation

Subsequently, the main structures for the neural networks used to estimate the pull-in voltage are provided. According to the above equation governing the static behavior of the micro-switch, it is clear that the pull-in voltage is a function of the following parameters: thickness h, length L, gap size G_1, Young’s modulus E, applied voltages ratio $p = V_2/V_1$, the width b. Thus, the proposed inputs to the ANNs will be the six above parameters. However, considering “Eq. (3)”, the normalizing parameter $\alpha = \varepsilon_0 b L^4 / 2EIG_1^3 = 6\varepsilon_0 L^4 / Eh^3 G_1^3$ is showing that the width parameter b has no direct effect on the pull-in voltage estimation of beam with rectangular cross section, as previously recommended in [45]. Accordingly, we suggest to restrain the number of inputs of the neural network to the following 5 parameter: h, L, g, E, p, nevertheless, and in order to validate the aforementioned recommendation, we will consider the 6 input states as well.

The designed neural networks are illustrated in “Fig. 2a.” and “Fig. 2b.” As shown in both figures, the respective ANNs designs consist of one input layer with 5 and 6 inputs, respectively, two hidden layers of 10 and 8 neurons, correspondingly, and an output layer of one output (the pull-in voltage). Transfer functions of the first and second hidden layers and the output layer are "tanget sigmoid", "log sigmoid", and "purelin", respectively [46].

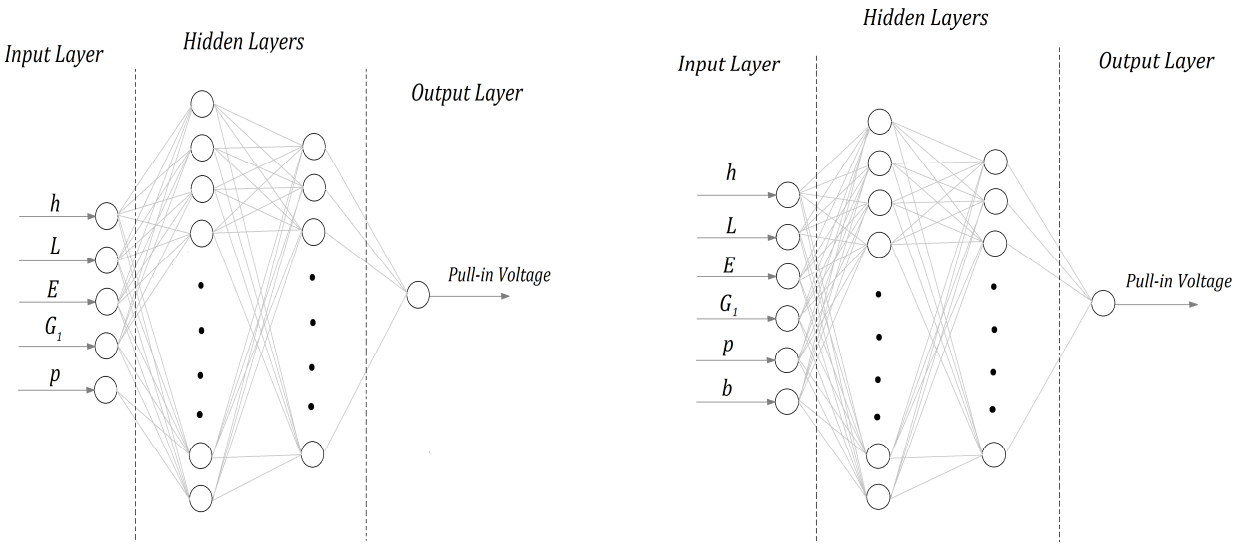

a. Designed Artificial Neural Network 1 (ANN1) with 5 inputs

b. Designed Artificial Neural Network 2 (ANN2) with 6 inputs

Fig. 2. Designed Neural network for estimating of pull-in voltage.

The number of neurons in each layer is determined based on trial and error, and the main criterion for selecting the number of neurons is Mean Square Error (MSE) minimization. In this way, different configurations for the structure of the neural network were analyzed and the most optimal configuration with 10 and 8 neurons in layers 1 and 2; has been selected. The maximum number of neurons for trial and error process was considered 20 neuron in each layer. It is noteworthy that the high number of neurons in a layer may causes of over fitting problem.

Selecting the number of ANN layers is the same as selecting the number of neurons, and is based on MSE minimization with trial and error procedure. This process was performed for single-layer, 2-layer and 3-layer modes, and the most optimal mode for this configuration was 2-layer mode. It should be noted that increasing the number of layers causes significant complexity of ANN, increases of train time, as well as over fitting problem.

As stated earlier, the proposed ANN network learning process is based on the Levenberg-Marquardt method [46]. The training included 280 samples with different and random values of the six input parameters as listed in Table (1). For the values randomization, the following domains were considered: $0.5\mu m \le h \le 4\mu m$, $50\mu m \le L \le 800\mu m$, $0.5\mu m \le G_1 \le 5\mu m$, $70GPa \le E \le 170GPa$, $2\mu m \le b \le 20\mu m$ and, $0 \le p \le 1$. These ranges are indeed suggesting reasonable values with respect to the design and size selection of such micro-structures. Next, the pull-in voltage of each sample was provided using the process presented in section (3) and tabulated in Table (1) as well. After the pull-in voltage was numerically estimated and the inputs and outputs of the neural networks were provided, the neural network-based voltage determined is also shown in Table (1). In this table, $\hat{y}_1$ and $\hat{y}_2$ are the output of the ANN schemes 1 and 2 (ANN1 and ANN2), respectively. Moreover, the efficiency of the neural networks is evaluated through determining the percentage of output error in form of $e_1\% = | y - \hat{y}_1 | / y \times 100\%$ and $e_2\% = | y - \hat{y}_2 | / y \times 100\%$ as summarized in Table (1). As seen in the table, the highest e_1 and e_2 values are respectively 5.71% and 9.89%. However, most of the errors e_1 and e_2 values are less than 1%. Also, the MSE value for neural networks 1 and 2, i.e., $MSE = 1/N \times \sum_{n=1}^{280} (e_i)^2$ are 1.4685×10^{-4} and 1.9791×10^{-4}, respectively. It is noteworthy that most of higher errors occur at voltages of lower than 2 volts.

The number of data has significant impact in minimizing of MSE and matching ANN output with test data. If the amount of data is less than specified limit; the above conditions are not well satisfied. In this paper, the number of data is considered as 280 samples. For ANN training, the number of data 100, 150, 230, 280, and 350 were considered, which values of 100, 150, 230 couldn't satisfy optimal condition. However, for the 280 and 330 samples, the optimality conditions were almost the same, but 280 samples were considered for the final training. It is noteworthy that increasing of samples has little effect on the efficiency of the ANN and may rises training time.

A general comparison of the maximum error and MSE indices indicates that ANN1 is slightly more capable than ANN2. However, this does not hold true for all cases, and as Table (1) illustrates, ANN2 have produced, in some cases, better results than those of ANN1. Also, the pull-in voltage and error percentage diagrams of 280 samples listed in Table (1) are schematically illustrated in "Fig. 3." and "Fig. 4.".

Next, the results of both ANN1 and ANN2 pull-in voltage estimations with different micro-structure cases as summarized in Table (2) are compared with the results published in references [43, 47]. Looking at the computed errors related to both neural networks, the ANN1 is to a certain extent better than the ANN2 method in accurately predicting the pull-in voltages.

Table 1. Microswitches specifications together with obtained pull-in voltages of micro-switches via numerical method and ANN1 and ANN2.

Number of sample	h (μm)	L (μm)	G_1 (μm)	E (GPa)	b (μm)	p	Obtained pull-in voltage with Numerical Method (V)	$\hat{y}_1$ (V)	$\hat{y}_2$ (V)	e_1 %	e_2 %
1	3.8	736	3.8	125	3.9	0.85	48.17	48.26	48.32	0.18	0.31
2	1.4	50	1.1	76	18.8	0.65	263.81	264.14	263.89	0.12	0.03
3	2.3	396	3.5	104	5.3	0.92	65.86	66	66.05	0.21	0.28
4	1.3	368	3.6	114	6.7	0.69	32.07	31.94	32.07	0.4	0
5	2.2	395	2.4	75	16.3	0.58	26.28	26.28	26.27	0	0.03
6	2.6	627	0.5	87	10.7	0.81	1.48	1.41	1.47	4.72	0.67
7	2.8	291	1.9	135	15.8	0.87	72.35	72.02	72.36	0.45	0.01
8	1.8	638	2.4	102	9.1	0.98	10.53	10.48	10.46	0.47	0.66
9	1.7	403	1.7	158	6.9	0	14.09	13.92	13.99	1.2	0.7
10	0.6	181	4.1	167	14.1	0.61	59.77	59.73	58.4	0.06	2.29
11	3.5	591	2.4	123	9.7	0.98	36.48	36.32	36.31	0.43	0.46
12	3.6	405	4.4	139	10.1	0.52	174.51	174.16	174.13	0.2	0.21
13	3.2	164	2.2	168	12.9	0.47	345.01	344.91	345.11	0.02	0.02
14	0.8	305	3.9	98	3	0.8	24.49	24.39	24.38	0.4	0.44
15	1.4	505	2.2	111	7.6	0.22	8.39	8.34	8.43	0.59	0.47
16	1.6	193	4.1	116	15.9	0.49	186.04	186.44	186.25	0.21	0.11
17	2.8	603	3.8	145	14.5	0.9	50.32	50.52	50.57	0.39	0.49
18	0.9	232	2.1	151	4.2	0.57	23.18	23.07	23.4	0.47	0.94
19	3	738	1.4	79	4.3	0.84	5.99	5.89	6.07	1.66	1.33
20	0.8	251	4	87	3.6	0.73	34.38	34.13	34.35	0.72	0.08
21	2.7	624	4.7	105	2.1	0.58	46.44	46.1	46.19	0.73	0.53
22	2.2	191	1.9	75	9.6	0.24	75.61	75.29	76.09	0.42	0.63
23	3.2	265	3.5	121	13.8	0.66	233.05	232.67	233.11	0.16	0.02
24	3	118	2.4	103	15	0.08	521.91	521.33	522	0.11	0.01
25	3.6	482	4.2	87	11.5	0.62	92.87	92.75	92.69	0.12	0.19
26	3.6	562	3.9	90	3.9	0.66	62.66	62.42	62.66	0.38	0
27	1.6	459	1.2	159	13.3	0.72	6.49	6.58	6.51	1.38	0.3
28	2.9	369	4.3	136	4.2	0.89	163.92	163.98	164.01	0.03	0.05
29	1.1	533	4.9	116	4.4	0.98	22.37	22.45	22.29	0.35	0.35
30	0.6	535	2.8	160	3.7	0.76	3.95	3.9	4.06	1.26	2.78
31	3.1	559	4.4	80	4.5	0.58	56.38	55.93	56.27	0.79	0.19
32	2.2	526	3.1	143	5	0.92	34.17	34.32	34.13	0.43	0.11
33	2.1	758	1.1	142	5.5	0.58	2.85	2.87	2.85	0.7	0
34	3.6	206	1.3	125	7.7	0.01	98.64	98.26	99.58	0.38	0.95
35	2.6	581	2.3	88	7.6	0.12	15.09	15	15.17	0.59	0.53
36	2.6	227	3.8	129	5.9	0.86	292.4	292.66	293.72	0.08	0.45
37	3.3	505	4	83	18	0.84	72.55	72.41	72.64	0.19	0.12
38	2.5	387	1.9	91	14.6	0.2	24.57	24.44	24.59	0.52	0.08
39	1.1	394	2.9	158	12	0.55	18.02	17.79	18.11	1.27	0.49
40	1.3	546	0.9	77	5.3	0.62	1.47	1.43	1.42	2.72	3.4
41	3.6	627	1	94	5.8	0.03	6.29	6.09	6.29	3.17	0
42	2.2	546	3.5	113	18.4	0.36	28.76	28.73	28.71	0.1	0.17
43	1	362	2.7	71	14.7	0.04	10.59	10.56	10.62	0.28	0.28
44	3.9	681	1.3	158	12	0.48	11.89	11.49	11.92	3.36	0.25
45	2.9	674	2.7	89	7.6	0.19	16.95	16.86	17.01	0.53	0.35
46	2.2	242	1.1	79	4.9	0.12	21.26	21.05	21.26	0.98	0
47	2.1	510	0.7	100	13.2	0.2	2.56	2.56	2.59	0	1.17
48	0.7	486	4.3	115	19.7	0.14	8.89	8.8	8.81	1.01	0.89
49	2.8	455	3	80	5	0.18	39.07	38.99	39.1	0.2	0.07
50	0.6	702	4.6	168	6.6	0.04	4.47	4.42	4.56	1.11	2.01
51	0.7	248	3.6	102	9.1	0.63	25.97	25.99	26.15	0.07	0.69
52	2.3	288	3.1	99	3.3	0.28	85.37	85.41	85.41	0.04	0.04
53	0.8	139	4.1	76	14.3	0.53	103.46	102.72	103.51	0.71	0.04
54	3.3	754	4.4	99	9.2	0.69	38.84	38.67	38.32	0.43	1.33
55	3.3	534	4.9	74	19.6	0.49	75.29	75.29	75.31	0	0.02
56	3	409	0.5	120	9.2	0.53	4.65	4.55	4.55	2.15	2.15
57	1	529	4.3	145	13.1	0.44	14.66	14.68	14.85	0.13	1.29
58	2.8	458	3.2	132	4.7	0.12	54.46	54.34	54.39	0.22	0.12
59	2.3	535	4.9	78	8.8	0.49	44.76	44.61	45.1	0.33	0.75
60	3.9	457	2.8	78	4.9	0.85	64.9	64.65	65.1	0.38	0.3
61	2.7	590	2.6	146	15.6	0.87	27.73	27.6	28.13	0.46	1.44
62	3.3	441	4.1	159	17.6	0.27	120.51	120.49	120.61	0.01	0.08
63	2	795	1.5	122	8.3	0.2	3.38	3.41	3.44	0.88	1.77
64	2	214	2.7	80	14.3	0.56	95.14	94.8	95.53	0.35	0.4
65	0.7	132	3	103	11.5	0.41	67.21	67.24	67.21	0.04	0
66	0.9	97	4.3	99	16.9	0.2	299.9	300.09	300	0.06	0.03
67	1.1	353	3.8	143	12.7	0.94	36.97	37.19	37.04	0.59	0.18
68	1.8	386	3.1	71	8	0.08	27.68	27.58	27.75	0.36	0.25
69	3.4	324	1.6	74	7.3	0.1	38.59	38.43	38.46	0.41	0.33
70	3.3	622	3.4	136	10.1	0.14	42.08	41.96	42.22	0.28	0.33
71	1.8	628	3.3	122	8.4	0.62	15.98	15.88	15.92	0.62	0.37
72	2.3	749	3.4	142	12	0.57	18.17	17.97	18.16	1.1	0.05
73	1.9	779	3.7	140	15.3	0.05	13.49	13.22	13.19	2	2.22
74	1.5	572	3.9	138	4.2	0.73	20.68	20.59	20.74	0.43	0.29
75	2	120	3.1	125	2.4	0.06	443.01	444.08	444	0.24	0.22

Table 1. Continued.

Number of sample	$h\ (\mu m)$	$L\ (\mu m)$	$G_1\ (\mu m)$	$E\ (GPa)$	$b\ (\mu m)$	p	Obtained pull-in voltage with Numerical Method (V)	$\hat{y}_1$ (V)	$\hat{y}_2$ (V)	e_1%	e_2%
76	0.5	444	4.6	109	7.2	0.86	7.99	7.99	8.19	0	2.5
77	3.9	447	3.1	76	7.7	0.93	81.93	81.8	82.05	0.15	0.14
78	1	695	0.5	147	13.7	0.98	0.42	0.4	0.46	4.76	9.52
79	0.8	413	1	103	19.2	0.85	1.82	1.8	1.64	1.09	9.89
80	1.8	345	4.3	130	18.8	0.78	85.96	85.46	85.86	0.58	0.11
81	1.1	553	2.6	143	10.2	0.51	7.31	7.3	7.33	0.13	0.27
82	2.2	605	4.3	80	6.3	0.17	26.5	26.19	26.42	1.16	0.3
83	1.6	440	1.4	82	15.7	0.39	5.94	5.96	6.04	0.33	1.68
84	3.8	310	2.9	124	15.6	0.13	157.04	156.87	158.11	0.1	0.68
85	3.7	162	3.3	118	15.3	0.03	653.87	653.3	654	0.08	0.01
86	3	246	3.2	149	3.9	0.3	224.52	224.55	224.59	0.01	0.03
87	1.4	83	2.1	142	14.2	0.29	324.01	324.49	325	0.14	0.3
88	1.9	616	0.7	75	10.3	0.33	1.32	1.29	1.33	2.27	0.75
89	2.4	232	2.7	77	5.8	0.46	102.62	102.72	102.62	0.09	0
90	3.7	381	1.3	78	3.7	0.64	25.49	25.38	25.42	0.43	0.27
91	1.9	565	1	149	16.8	0.02	3.71	3.7	3.67	0.26	1.07
92	3.9	319	1.4	163	5.1	0.84	67.76	67.54	69.64	0.32	2.77
93	1.5	602	1.1	137	4.9	0.55	2.66	2.69	2.66	1.12	0
94	2.9	346	1.3	83	13.9	0.85	23.78	23.65	22.2	0.54	6.64
95	2.8	562	0.6	141	18	0.34	3.09	3.01	2.98	2.58	3.55
96	2.3	578	3.3	80	11.2	0.44	21.39	21.37	21.38	0.09	0.04
97	2.9	381	1.7	81	14.6	0.05	25.18	24.89	25.17	1.15	0.03
98	1.1	298	3.6	102	19.1	0.66	35.65	35.52	35.79	0.36	0.39
99	0.9	368	2.7	134	11.7	0.33	13.09	12.38	12.62	5.42	3.59
100	3.9	252	2.9	144	14.2	0.89	312.9	312.73	313.01	0.05	0.03
101	1	197	2.5	127	2.6	0.11	42.54	42.43	42.53	0.25	0.02
102	0.6	666	1	143	16.5	0.97	0.58	0.57	0.56	1.72	3.44
103	2.4	372	2.7	93	15.4	0.53	44.5	44.3	44.57	0.44	0.15
104	3.5	715	4.3	142	4.1	0.7	54.66	54.24	54.58	0.76	0.14
105	2.8	343	4.4	166	11.4	0.99	226.9	226.76	226.99	0.06	0.03
106	1.1	626	1.7	155	7.8	0.28	3.05	3.14	3.02	2.95	0.98
107	1.7	347	1.4	78	11.8	0.41	10.29	10.25	10.45	0.38	1.55
108	2.1	656	3	106	9.1	1	18.68	18.31	18.27	1.98	2.19
109	3.9	616	3.3	106	9.4	0.76	51.33	50.93	51.39	0.77	0.11
110	1	333	2.3	137	5.2	0.81	15.49	15.49	15.31	0	1.16
111	3.4	212	1.4	129	6.5	0.1	97.81	97.37	97.93	0.44	0.12
112	2.7	642	4.7	148	2.3	0.17	49.54	49.4	50.23	0.28	1.39
113	1.8	761	0.8	106	18.6	0.35	1.16	1.17	1.16	0.86	0
114	1.1	295	0.9	90	13.7	0.05	3.98	4.07	3.95	2.26	0.75
115	1.9	553	1.1	78	18.7	0.52	3.37	3.36	3.29	0.29	2.37
116	2.1	378	1.2	146	4.9	0.33	12.76	12.89	12.96	1.01	1.56
117	0.9	675	3.2	90	18.5	0.17	3.79	3.91	3.93	3.16	3.69
118	2.5	626	3	108	16.3	0.2	20.25	20.19	20.07	0.29	0.88
119	1.8	696	4.6	92	9.9	0.67	18.89	18.73	18.94	0.84	0.26
120	2.5	792	3.7	133	6.6	0.46	19.78	19.68	19.85	0.5	0.35
121	1.3	435	3.8	117	15.5	0.91	27.65	27.81	27.85	0.57	0.72
122	1.5	713	0.7	85	6.1	0.1	0.72	0.7	0.71	2.77	1.38
123	2.6	491	4.3	147	3.1	0.74	76.45	75.84	76.45	0.79	0
124	1.4	166	4.7	79	15.8	0.73	220.52	220.64	220.6	0.05	0.03
125	3.9	355	4.3	93	14.8	0	194.9	194.38	195.96	0.26	0.54
126	3	611	4	122	13.5	0.59	48.08	47.86	47.87	0.45	0.43
127	1.7	669	2.8	79	9.5	0.29	7.78	7.72	7.9	0.77	1.54
128	2.5	642	1.2	110	9	0.13	4.91	4.95	4.91	0.81	0
129	0.8	288	2.2	80	16.6	0.21	9.38	9.38	9.5	0	1.27
130	3.6	450	1.1	81	7.7	0.89	15.29	15.13	15.45	1.04	1.04
131	3.5	117	0.6	147	16.6	0.07	99.71	99.53	99.8	0.18	0.09
132	1.4	152	1.8	129	17.3	1	97.17	98.56	97.21	1.43	0.04
133	2.5	558	1.8	165	11.1	0.44	15.08	14.66	15	2.78	0.53
134	0.5	421	1.9	112	13.4	0.01	2.05	2.04	1.99	0.48	2.92
135	1.9	192	2.6	138	19.1	0.89	152.01	151.93	152.37	0.05	0.23
136	1.5	421	3.4	145	9.9	0.19	29.19	29.15	29.07	0.13	0.41
137	1	160	0.6	112	3	0.09	7.12	7.05	7.12	0.98	0
138	1	467	4.2	101	14.4	0.92	17.65	17.73	17.83	0.45	1.01
139	2.7	415	0.8	121	2.5	0.71	8.18	8.12	8.36	0.73	2.2
140	2.8	561	4	88	2.7	0.22	41.54	41.32	41.6	0.52	0.14
141	1.9	702	1.7	155	13.1	0.86	6.3	6.4	6.37	1.58	1.11
142	3.2	505	4.4	140	10.9	0.4	92.93	92.81	93.09	0.12	0.17
143	3.3	318	0.6	111	10.2	0.96	13.38	13.27	13.48	0.82	0.74
144	1.1	56	2.9	108	3.9	0.76	773.86	774.07	774	0.02	0.01
145	2.7	546	4.9	128	19.2	0.36	68.87	68.84	68.99	0.04	0.17
146	1.1	391	0.5	108	7.7	0.33	1.05	0.99	1.07	5.71	1.9
147	1.4	445	4	133	9	0.19	28.78	28.96	28.63	0.62	0.52
148	3.2	198	1.1	70	6.5	0.09	52.15	51.75	52.81	0.76	1.26
149	1.6	369	3	132	6.8	0.11	32.88	32.79	33.01	0.27	0.39
150	1.4	250	4.2	92	18.9	0.59	85.43	85.41	86.07	0.02	0.74

Table 1. Continued.

Number of sample	h (μm)	L (μm)	G_1 (μm)	E (GPa)	b (μm)	p	Obtained pull-in voltage with Numerical Method (V)	$\hat{y}_1$ (V)	$\hat{y}_2$ (V)	e_1 %	e_2 %
151	0.7	529	2.8	117	6.8	0.08	3.93	3.96	3.88	0.76	1.27
152	3.2	524	4.2	121	17.3	0.81	82.47	82.12	82.39	0.42	0.09
153	1.9	579	1.1	99	11.6	0.23	3.35	3.35	3.33	0	0.59
154	2.8	123	3.4	102	3	0.02	725.86	725.23	726.01	0.08	0.02
155	1	660	0.7	151	15.6	0.94	0.82	0.78	0.78	4.87	4.87
156	2.7	242	3.9	102	17.7	0.24	219.57	219.59	219.6	0	0.01
157	1.7	477	2.9	84	4.9	0.53	17.09	17.09	17.03	0	0.35
158	1.5	563	4.1	80	14.6	0.88	18.67	18.79	18.74	0.64	0.37
159	3.7	440	1.9	108	14.2	0.3	37.58	37.66	37.68	0.21	0.26
160	3.3	265	3.3	150	7.8	0.08	231.7	231.25	231.8	0.19	0.04
161	2.5	128	3.7	130	8.8	0.57	761.6	761.95	762	0.04	0.05
162	3.1	111	1	93	16.8	0.69	171.08	170.97	171.1	0.06	0.01
163	2.8	498	2.7	123	4.7	0.76	38.19	37.86	38.39	0.86	0.52
164	3.1	228	2	91	17.4	0.28	105.93	105.55	106.09	0.35	0.15
165	3.6	686	1.8	167	13	0.2	16.88	16.54	16.9	2.01	0.11
166	3.6	493	3.7	105	18.8	0.57	79.74	79.74	79.63	0	0.13
167	2	547	1.2	90	8.8	0.76	4.84	4.82	4.82	0.41	0.41
168	0.5	395	3.7	141	2.3	0.06	7.19	7.34	7.3	2.08	1.52
169	1.2	202	1.3	119	2.9	0.06	19.38	19.56	19.12	0.92	1.34
170	3.7	210	2.6	95	8.9	0.95	299.71	299.42	302.26	0.09	0.85
171	3.9	508	0.8	129	12.3	0.85	10.38	10.11	10.8	2.6	4.04
172	0.6	731	4.6	120	19.5	0.42	3.58	3.63	3.57	1.39	0.27
173	2.9	452	2.9	154	19.2	0.94	66.78	66.48	66.78	0.44	0
174	1.1	218	1.8	113	10.5	0.47	23.87	23.9	24.53	0.12	2.76
175	2.3	234	0.9	149	10.9	0.14	24.69	24.82	24.52	0.52	0.68
176	2	457	4.5	129	16.5	0.55	56.94	56.91	57.23	0.05	0.5
177	1.7	404	3.3	89	9	0.4	29.18	29.23	29.15	0.17	0.1
178	2.4	137	3.4	148	19.5	0.45	575.91	575.83	576	0.01	0.01
179	2.9	166	2	84	9.7	0.5	178.31	177.94	178.42	0.2	0.06
180	1.1	273	3.8	84	10.6	0.48	40.28	40.41	40.07	0.32	0.52
181	1.9	147	0.6	139	13.8	0.38	25.18	24.84	25.23	1.35	0.19
182	2.3	463	1.9	115	7.2	0.34	17.29	17.19	17.39	0.57	0.57
183	3.8	555	3.8	133	13.1	0.01	75.9	75.71	76.11	0.25	0.27
184	3.9	429	2.6	94	5.8	0.9	74.48	74	74.46	0.64	0.02
185	3.1	737	2.5	70	17.2	0.81	13.95	13.83	14.03	0.86	0.57
186	2.9	794	4.2	148	15.3	0.37	30.91	31.04	31.07	0.42	0.51
187	1.3	705	2	129	18	0.49	3.68	3.73	3.64	1.35	1.08
188	2.8	576	1.6	85	19.7	0	9.78	9.71	9.78	0.71	0
189	1.5	394	3.4	144	11.1	0.39	33.67	33.73	33.51	0.17	0.47
190	1.6	561	3.7	88	5.7	0.39	16.28	16.32	16.14	0.24	0.85
191	1.8	206	4.7	102	5.1	0.61	229.67	229.76	229.72	0.03	0.02
192	3.1	771	4.5	122	5	0.12	35.88	35.59	35.81	0.8	0.19
193	2.5	701	0.7	146	18.7	0.85	2.43	2.43	2.54	0	4.52
194	0.5	86	4.9	136	6.1	0.36	227.67	227.55	227.71	0.05	0.01
195	0.6	478	3.2	107	11.3	0.91	5.31	5.43	5.32	2.25	0.18
196	2.1	752	4.4	149	16.6	0.48	23.28	23.17	23.39	0.47	0.47
197	2.1	251	3.8	135	19.9	0.08	153.71	153.59	153.93	0.07	0.14
198	1.1	577	1.6	132	3.8	0.03	2.99	3.06	2.92	2.34	2.34
199	3.5	646	5.5	165	12.3	0.99	124.47	124.03	124.54	0.35	0.05
200	3.5	57	0.5	104	6.6	0.79	347.47	347.62	347.5	0.04	0
201	1.4	551	3.8	113	18	0.09	15.98	15.9	15.77	0.5	1.31
202	3.2	374	2.8	95	5.6	0.91	82.37	82.3	82.4	0.08	0.03
203	1.5	83	1.6	98	2.5	0.79	221.11	220.35	221.2	0.34	0.04
204	3.9	673	3.5	127	19.7	0.53	48.47	48.14	48.45	0.68	0.04
205	1.2	196	5	96	15.5	0.44	142.73	142.77	142.77	0.02	0.02
206	2.5	367	3.6	81	17.4	0.73	73.35	73.08	73.25	0.36	0.13
207	1.7	339	4.9	122	12.7	0.1	85.76	85.62	85.86	0.16	0.11
208	2.2	220	4.6	101	19.3	0.63	263.92	263.49	263.99	0.16	0.02
209	1.8	404	3.3	79	17.4	0.08	29.29	29.05	29.24	0.81	0.17
210	2.7	485	4.5	114	12	0.62	75.68	75.19	75.57	0.64	0.14
211	1.3	196	2.5	99	19.3	0.47	58.08	57.85	58.29	0.39	0.36
212	0.9	680	5.7	86	12.9	0.34	8.77	8.85	8.78	0.91	0.11
213	2.2	150	1.1	85	4.6	0.23	57.48	57.45	57.5	0.05	0.03
214	1.2	594	5.4	112	5.8	0.6	19.48	19.42	19.6	0.3	0.61
215	3.2	752	4.9	149	2.8	0.28	50.16	50.15	50.32	0.01	0.31
216	1.2	423	2.9	96	4.3	0.44	13.58	13.61	13.66	0.22	0.58
217	3.3	461	0.9	101	17	0.62	9.52	9.48	9.62	0.42	1.05
218	2.4	687	4.8	88	14.2	0.82	32.67	32.63	32.92	0.12	0.76
219	2.4	558	4.2	122	5.8	0.07	42.04	41.68	42.04	0.85	0
220	2.8	354	2.5	145	7	0.5	68.36	68.15	68.43	0.3	0.1
221	0.9	577	4.1	165	2	0.29	10.24	10.21	10.35	0.29	1.07
222	1.9	82	1.3	78	5.8	0.8	43.1	43.3	43.1	0.46	0
223	0.7	496	3.1	143	6	0.85	6.65	6.67	6.77	0.3	1.8
224	0.6	448	1.8	132	3.2	0.08	2.39	2.43	2.37	1.67	0.83
225	2	604	5.5	97	5.2	0.16	36.57	36.5	36.77	0.19	0.54

Table 1. Continued.

Number of sample	$h\ (\mu m)$	$L\ (\mu m)$	$G_1\ (\mu m)$	$E\ (GPa)$	$b\ (\mu m)$	p	Obtained pull-in voltage with Numerical Method (V)	$\hat{y}_1\ (V)$	$\hat{y}_2\ (V)$	$e_1\%$	$e_2\%$
226	3.3	503	2.5	80	3.1	0.34	31.56	31.39	31.5	0.53	0.19
227	0.9	750	5	79	17.5	0.34	5.68	6	5.68	5.63	0
228	1.4	97	1.2	152	18	0.56	110.71	110.82	110.8	0.09	0.08
229	3.4	678	3.3	78	13.4	0.4	27.39	27.04	27.33	1.27	0.21
230	1.5	346	4.2	117	10.8	0.47	54.78	54.86	54.96	0.14	0.32
231	1.3	377	3.2	166	16.1	0	28.49	28.21	28.57	0.98	0.28
232	1.3	168	1.7	140	10.6	0.74	56.05	56.29	56.03	0.42	0.03
233	1.6	589	4.5	100	17.4	0.44	21.28	21.3	21.2	0.09	0.37
234	2.1	789	2	94	19.5	0.66	5.39	5.29	5.33	1.85	1.11
235	2.9	731	1.1	132	6.8	0.59	4.89	4.76	4.82	2.65	1.43
236	2.8	169	2.3	160	17	0.76	296.21	296.05	296.3	0.05	0.03
237	2.9	453	5.9	150	16	0.44	160.62	160.39	160.74	0.14	0.07
238	1.4	435	1.5	166	13.9	0.71	8.39	8.49	8.4	1.19	0.11
239	1	117	1.6	95	18.8	0.47	55.17	54.41	55.2	1.37	0.05
240	2.4	790	1.2	111	6	0.51	3.18	3.23	3.26	1.57	2.51
241	1.5	318	2.9	133	9.5	0.62	40.78	40.57	40.38	0.51	0.98
242	3.8	695	4.6	82	2.2	0.7	55.06	54.43	55.18	1.14	0.21
243	2.6	511	3.8	76	7	0.75	42.38	42.23	42.62	0.35	0.56
244	2.5	692	1.4	102	15.3	0	5.19	5.09	5.2	1.92	0.19
245	1.5	365	1.5	85	3.4	0.39	8.89	8.88	9.05	0.11	1.79
246	0.8	451	4.5	86	16.3	0.82	13.39	13.01	13.21	2.83	1.34
247	2.7	173	1.3	134	13.5	0.67	101.21	101.47	101.57	0.25	0.35
248	3.4	666	5	90	8.5	0.97	69.64	69.58	69.61	0.08	0.04
249	1.4	291	2.9	111	17.3	0.02	37.66	37.37	37.72	0.77	0.15
250	1.9	171	1.1	160	17.6	0.58	50.67	51.09	50.75	0.82	0.15
251	2.1	417	2.7	96	3	0.37	28.68	28.71	28.83	0.1	0.52
252	3.9	798	4.9	164	7.9	0.14	62.38	61.92	62.34	0.73	0.06
253	1.3	573	1.7	128	12	0.46	4.34	4.37	4.33	0.69	0.23
254	2	489	3.4	164	4.1	0.46	36.28	35.78	35.81	1.37	1.29
255	1.6	462	1.3	118	6.9	0.55	5.94	5.97	6.05	0.5	1.85
256	1.3	646	5	88	13.6	1	18.39	18	18.11	2.12	1.52
257	2.9	183	1	144	11.1	0.35	66.63	66.78	66.62	0.22	0.01
258	2.3	265	2.4	162	2	0.43	89.32	88.43	89.44	0.99	0.13
259	1.3	220	2.9	80	4.1	0.49	51.86	52.11	51.93	0.48	0.13
260	2.4	408	1.4	153	19	0.79	18.98	18.69	19	1.52	0.1
261	3.8	368	4.4	128	7.1	0.9	249.72	249.57	249.8	0.06	0.03
262	1.8	278	2.4	108	18.9	0.98	56.84	56.68	54.82	0.28	3.55
263	0.8	683	5.4	125	13.1	0.12	8.08	8	8.01	0.99	0.86
264	1.2	224	4.4	168	9.2	0.16	116.22	116.34	116.29	0.1	0.06
265	2.2	495	4.1	139	5.8	0.12	48.36	48.11	48.35	0.51	0.02
266	1	207	2.3	151	15.7	0.14	37.18	37.24	37.2	0.16	0.05
267	1	280	1.9	164	4.5	0.48	16.49	16.65	16.35	0.97	0.84
268	3	638	5.8	93	15.4	0.1	63.68	63.38	63.55	0.47	0.2
269	3.7	609	5.7	90	13	0.31	92.87	92.41	92.62	0.49	0.26
270	3	268	1.3	154	18.1	0.63	52.47	52.13	52.46	0.64	0.01
271	1.1	255	3.3	76	10.5	0.86	39.68	39.6	39.69	0.2	0.02
272	3.6	414	1.3	110	13.1	0.32	23.29	23.58	23.35	1.24	0.25
273	0.8	371	1.6	75	10.6	1	4.49	4.49	4.35	0	3.11
274	2.3	258	3.5	162	18.4	0.85	185.61	185.85	185.71	0.12	0.05
275	1.1	551	3.8	135	7.9	0.03	12.1	12.12	12.12	0.16	0.16
276	3.3	588	2.9	156	7.2	0.89	46.58	46.47	47.13	0.23	1.18
277	2.1	383	1.6	148	4.8	0.23	19.08	19.07	19.21	0.05	0.68
278	3.3	223	1.4	167	4.5	0.44	98.15	97.92	98.22	0.23	0.07
279	3	170	2.2	126	8.2	0.76	269.53	270.07	269.59	0.2	0.02
280	3.1	300	0.7	168	6.1	0.26	17.28	17.31	17.31	0.17	0.17

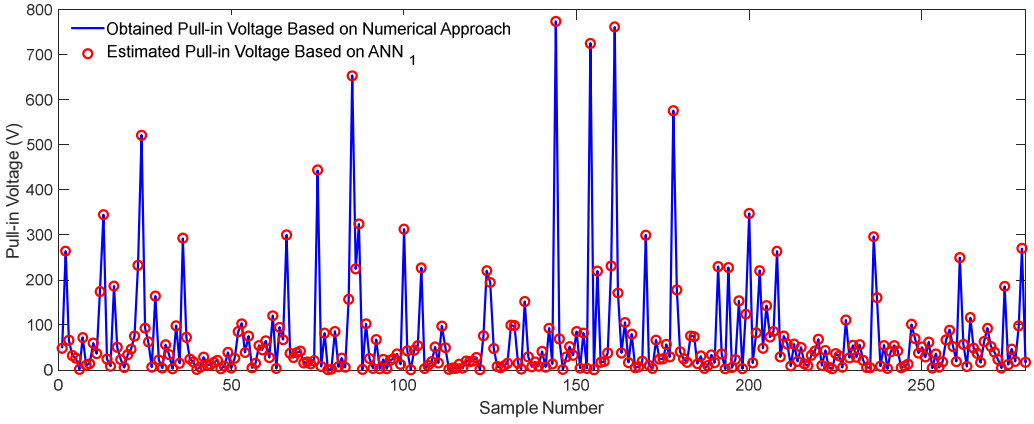

a. Obtained pull-in voltage via numerical method VS ANN1 for 280 samples

Fig. 3. Obtained pull-in voltage and error percentage using ANN1 for 280 samples listed in Table (1).

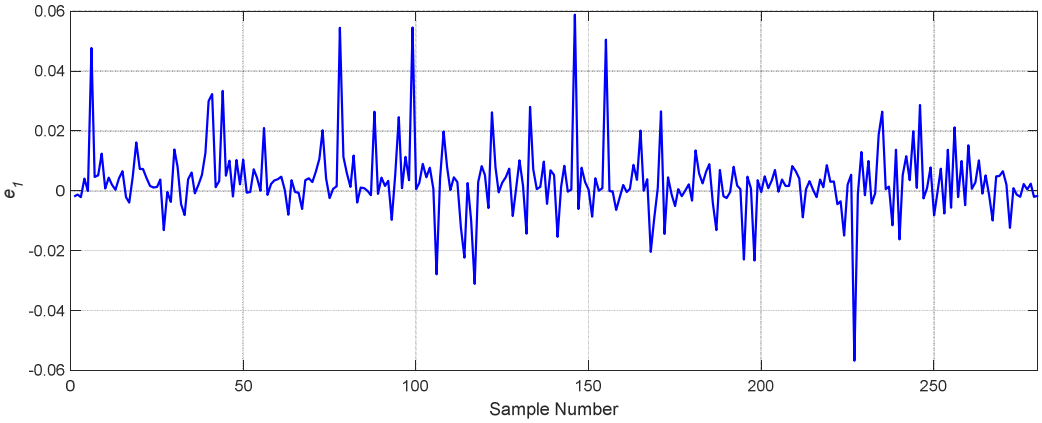

b. Calculated error percentage of ANN1 ($e_1 = | y - \hat{y}_1 | / y$) for 280 samples

Fig. 3. Continued.

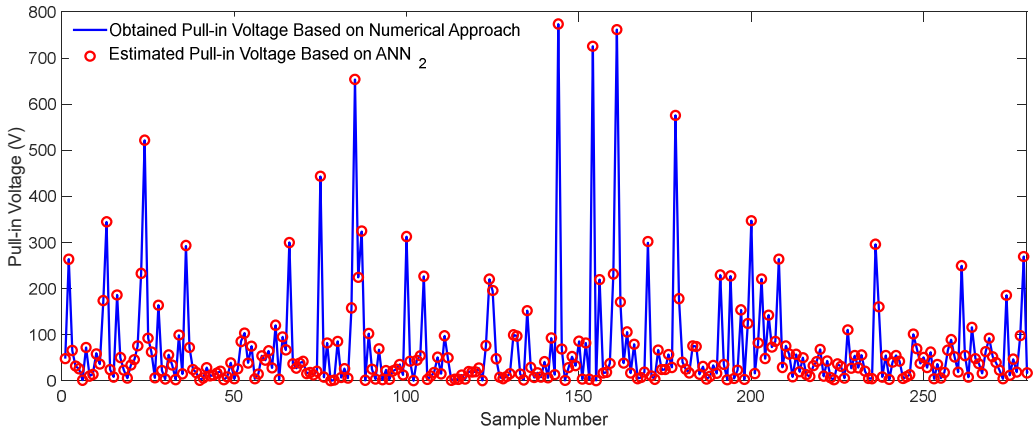

a. Obtained pull-in voltage via numerical method VS ANN2 for 280 samples

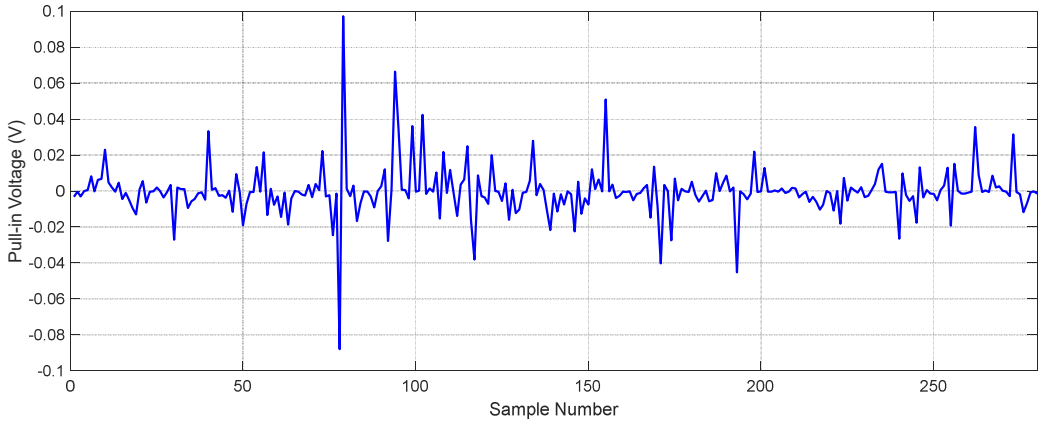

b. Calculated error percentage of ANN2 ($e_2 = | y - \hat{y}_2 | / y$) for 280 samples

Fig. 4. Obtained pull-in voltage and error percentage using ANN2 for 280 samples listed in Table (1).

To further extend the numerical validation, a micro-structure with following geometrical properties: $h = 3\mu m$, $G_1 = 1\mu m$, Young's modulus $E = 169GPa$, $b = 50\mu m$ and $p = 0$ is considered. Two length cases are also considered: $L = 250\mu m$ and $L = 350\mu m$. The results from previous works and those obtained using ANN1 and ANN2 are summarized in Table (3). As can be seen, both networks shows good agreement in estimating the pull-in voltage in a better and shorter time-frame.

Table 2. Comparison of obtained voltages obtained in refs. [43, 47] with obtained ones using ANN1 and ANN2 for various micro-switches

Case number	$h(\mu m)$	$L(\mu m)$	$G_1(\mu m)$	$E(GPa)$	$b(\mu m)$	p	Obtained pull-in voltage in refs. [43, 47]	$\hat{y}_1(V)$	$e_1\%$	$\hat{y}_2(V)$	$e_2\%$
1 [43]	2	600	2	169	8	1	14.04	14.13	0.64	13.62	2.99
2 [43]	2	600	2	169	8	0	10.54	10.36	1.70	10.62	0.76
3 [43]	2	600	5	169	8	0	42.25	41.96	0.68	42.45	0.47
4 [43]	2	600	5	169	8	0.6	44.75	44.63	0.27	45.52	1.72
5 [43]	2	600	5	169	8	0.8	47.5	47.75	0.52	48.48	2.06
6 [43]	2	600	5	169	8	0.94	51.91	52.77	1.66	52.78	1.67
7 [47]	2	400	1	169	10	1	11.21	11.04	1.51	11.01	1.78

Table 3. Comparison of obtained voltages of previous studies with obtained ones using ANN1 and ANN2 for micro-switches with $h = 3\mu m$, $G_1 = 1\mu m$, $E = 169GPa$, $b = 50\mu m$ and $p = 0$.

	$L = 250\mu m$	$L = 350\mu m$
Rokni et al. [48]	39.4	20.10
Haluzan et al. [49]	39.56	20.19
Sadeghian et al. [50]	39.13	20.36
Vakili-Tahami et al. [45]	-------	20.25
Rezazadeh et al. [51]	-------	20.2
ANN1	40.08	20.62
ANN2	39.21	20.01

Next, the effect of the system's specifications on the pull-in voltage is examined. The effect of such parameters as thickness, length, initial gap, Young's modulus, p and width are illustrated in "Figs 5-10.", respectively. As shown in "Figs. 5, 7-9.", as the thickness increases, the initial distance, Young's modulus, p as well as the pull-in voltage increase. As seen in "Figs. 5-10.", the ANN1 method estimates the pull-in voltage values for various parameters with a very good approximation. Also, "Fig. 8." suggests that the ANN2 method estimates the pull-in voltage for the following two cases: $E = 70GPa$ and $E = 169GPa$ with a low accuracy. Similarly, as shown in "Fig. 6.", as the length increases, the pull-in voltage decreases, and the significant point in this figure is the low capability of the ANN2 neural network to estimate the pull-in voltage for $L = 100\mu m$. However, concerning the other cases, the network showed an acceptable capability in estimating the pull-in voltage. As shown in "Figs. 5-10.", it is concluded that although the ANN2 method estimates the pull-in voltage well in most of the examined cases, it has significant errors in certain cases. In addition, it was found that the neural ANN1 method generally estimates with good accuracy the pull-in voltage for different cases. Thus, the ANN1 method is preferred to be used to estimate the pull-in voltage.

Finally, "Fig. 10." shows the pull-in voltage dependency with the micro-beam width changes. As mentioned before, the pull-in voltage of micro-structures should be independent of the width variation. According to the results of "Fig. 10.", the pull-in voltage slightly varies with the increasing width via the ANN2 neural method.

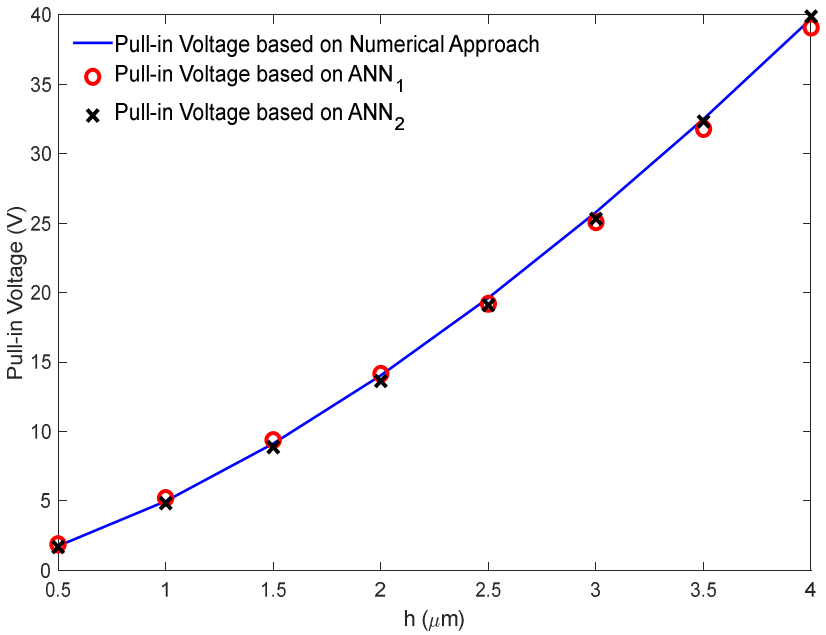

Fig. 5. Compassion of obtained pull-in Voltages via numerical approach vs. obtained ones using ANN1 and ANN2 for micro-switches with different thicknesses, $L = 600\mu m$, $G_1 = 2\mu m$, $E = 169GPa$, $b = 8\mu m$ and $p = 1$.

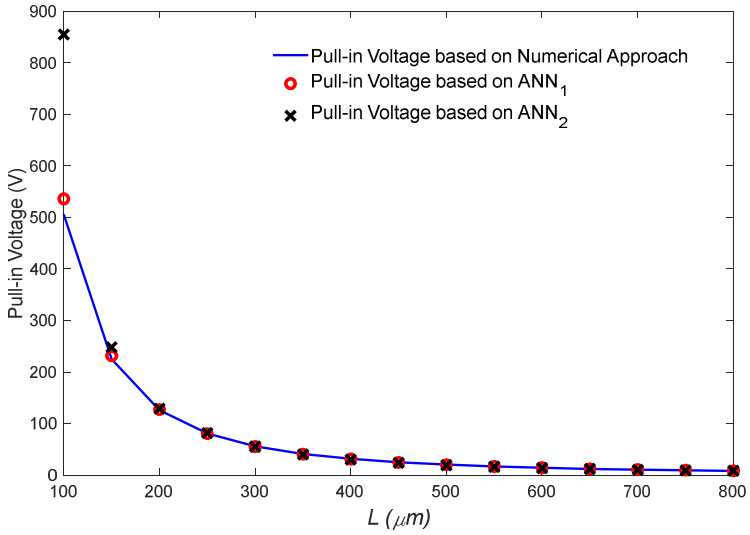

Fig. 6. Compassion of obtained pull-in Voltages via numerical approach vs. obtained ones using ANN1 and ANN2 for micro-switches with different lengths, $h = 2\mu m$, $G_1 = 2\mu m$, $E = 169GPa$, $b = 8\mu m$ and $p = 1$.

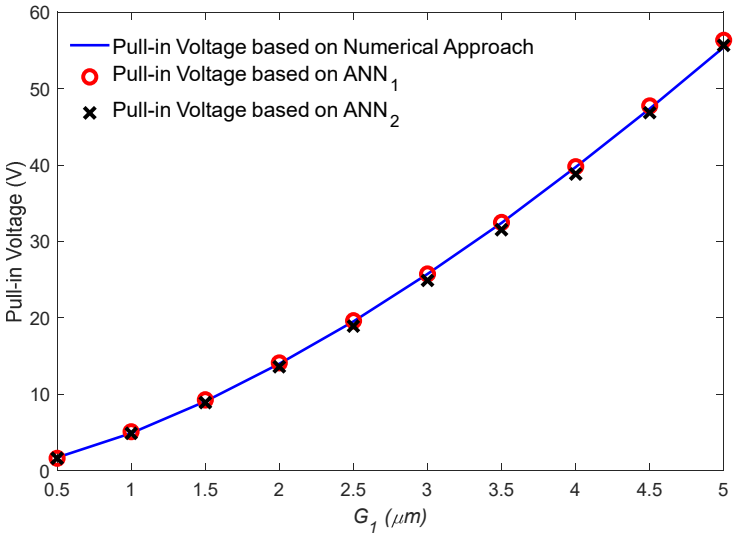

Fig. 7. Compassion of obtained pull-in Voltages via numerical approach vs. obtained ones using ANN1 and ANN2 for micro-switches with different initial gaps, $h = 2\mu m$, $L = 600\mu m$, $E = 169GPa$, $b = 8\mu m$ and $p = 1$.

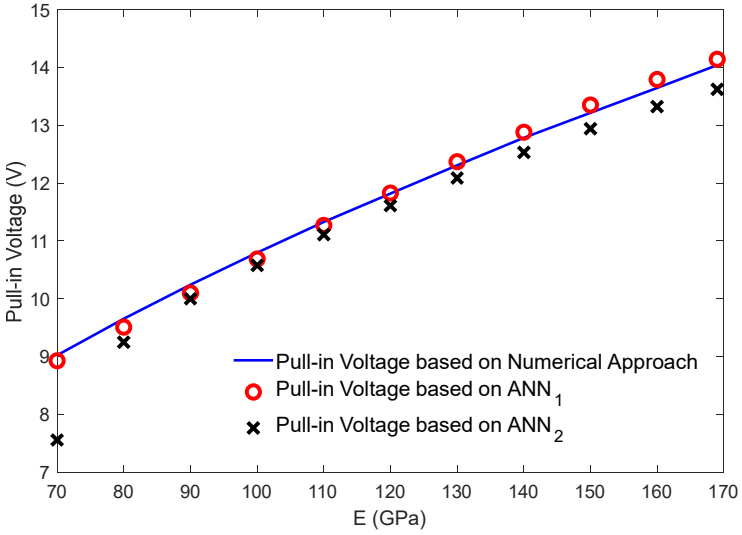

Fig. 8. Compassion of obtained pull-in Voltages via numerical approach vs. obtained ones using ANN1 and ANN2 for micro-switches with different Young modulus, $h = 2\mu m$, $L = 600\mu m$, $G_1 = 2\mu m$, $b = 8\mu m$ and $p = 1$.

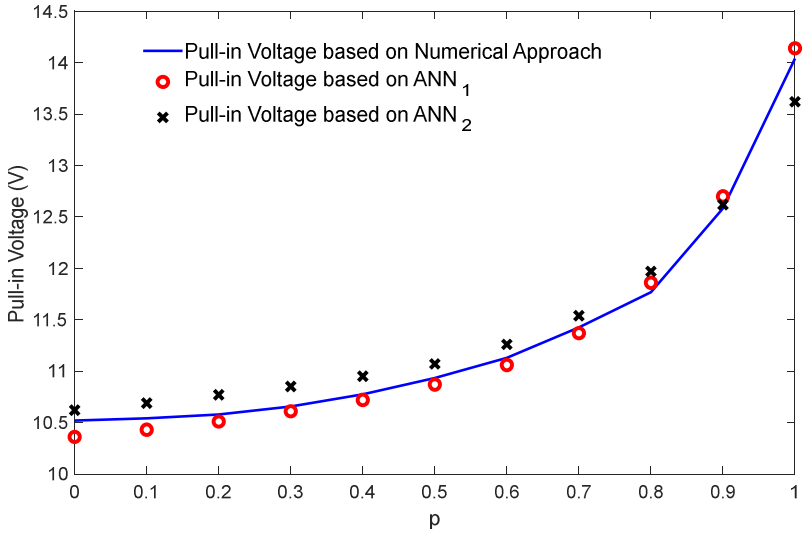

Fig. 9. Compassion of obtained pull-in Voltages via numerical approach Vs. obtained ones using ANN1 and ANN2 for micro-switches with different parameter of p, $h = 2\mu m$, $L = 600\mu m$, $G_1 = 2\mu m$, $E = 169GPa$ and $b = 8\mu m$.

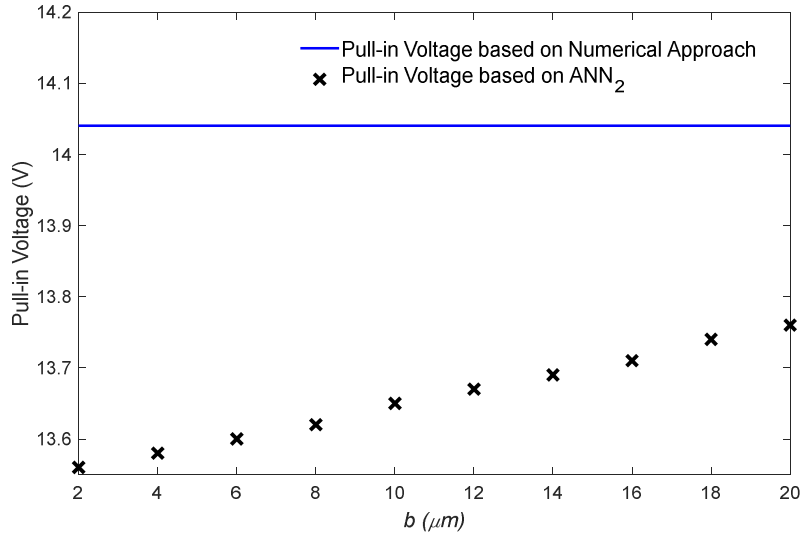

Fig. 10. Compassion of obtained pull-in Voltages via numerical approach Vs. obtained ones using ANN2 for micro-switches with different widths $h = 2\mu m$, $L = 600\mu m$, $G_1 = 2\mu m$, $E = 169GPa$ and $p = 1$.

5. Conclusion

Considering the significance of examining pull-in instability and determining pull-in voltage in micro-switches and micro-actuators, this paper sought to design neural networks to determine pull-in voltage of micro-switches. Designed neural networks are of two types; the first type doesn't consider the micro-switch width parameter as the input while the second one involves the width parameter. The type of neural networks employed is of feed forward back propagation, and the learning process of neural networks is based on the Levenberg-Marquardt method. The number of hidden layers and of neurons in each layer were determined by trial-and-error method and the best neural networks state were selected. Thus, the most optimal state includes two hidden layers and the number of 10 and 8 neurons in the first and second hidden layers. For this end, 280 data were taken up for training neural networks as pull-in voltage for micro-switches of different physical and geometric specifications. The required pull-in voltages for training process were determined using the SSLM method in conjunction with the Galerkin method, seen to be a reliable process for pull-in voltage determination.

After the neural networks training, their efficiency is evaluated through the percentage of output error and mean square error. As reported in the body of paper, the highest e_1 and e_2 values are respectively 5.71% and 9.89% for ANN1 and ANN2. It should be mentioned that, most of the errors e_1 and e_2 values are less than 1% and most of higher errors relate to pull-in voltages of less than 2 volts. Also, the calculated MSE value for ANN1 and ANN2 are 1.4685×10^{-4} and 1.9791×10^{-4}, respectively. Regarding to validation of designed networks, their performance was checked via comparing estimated values of pull-in voltage with those provided in previous references. This comparison indicates the good capability of designed neural networks to determine the pull-in voltage. Also, the effect of physical and geometrical specifications of micro-switches on voltage instability was examined, suggesting very good result generated by the neural network of ANN1 in general. However, in some rare cases, the neural network of ANN2 provided voltage instability with significant deviation. Finally, the neural network ANN1 was proposed to determine the pull-in voltage.

Author Contributions

M. Aliasghary initiated the project, and suggested the current research as well as ANN; H. Mobki developed the mathematical modeling and designed the ANN structure; H.M. Ouakad analyzed the pull-in study. The manuscript was written through the contribution of all authors. All authors discussed the results, reviewed, and approved the final version of the manuscript.

Acknowledgments

The authors greatly appreciate the editor and anonymous reviewers who have dedicated their considerable time and expertise to enhance this paper with constructive and valuable comments.

Conflict of Interest

The authors declared no potential conflicts of interest concerning the research, authorship, and publication of this article.

Funding

The authors received no financial support for the research, authorship, and publication of this article.

Data Availability Statements

The datasets generated and/or analyzed during the current study are available from the corresponding author on reasonable request.

References

[1] Perlmutter, M., Breit. S., *The future of the MEMS inertial sensor performance, design and manufacturing*, IEEE, Intertial sensors and systems (ISS), in DGON, 2016.
[2] Pitchappa, P., Manjappa, M., Ho, C.P., Singh, R., Singh, N., Lee, C., Active control of electromagnetically induced transparency analog in terahertz MEMS metamaterial, *Advanced Optical Materials*, 4(4), 2016, 541-547.
[3] Mobki, H., Majidzadeh Sabegh, A., Azizi, A., Ouakad, H.M., On the implementation of adaptive sliding mode robust controller in the stabilization of electrically actuated micro-tunable capacitor, *Microsystem Technologies*, 26, 2020, 3903-3916.
[4] Mobki, H., Jalilirad, M., Vatankhah Moradi, M., Azizi, A., Multi input versus single input sliding mode for closed-loop control of capacitive micro structures, *SN Applied Sciences*, 1(7), 2019, 1-13.
[5] Zhou, Q., Sussman, A., Chang, J., Dong, J., Zettl, A., Mickelson, W., Fast response integrated MEMS microheaters for ultra low power gas detection, *Sensors and Actuators A: Physical*, 223, 2015, 67-75.
[6] Choudhary, V., Iniewski, K., *Mems: fundamental technology and applications*, CRC Press, New York, 2017
[7] Liu, H., Zhang, L., Li, K.H.H., Tan, O.K., Microhotplates for metal oxide semiconductor gas sensor applications Towards the CMOS-MEMS monolithic approach, *Micromachines*, 9(11), 2018, 557.
[8] Mishra, M.K., Dubey, V., Mishra, P. M., Khan, I., MEMS technology: A review, *Journal of Engineering Research and Reports*, 4(1), 2019, 1-24.
[9] Mobki, H.,,Rashvand, K., Rezazadeh, G., Afrang, S., Sadegh, H.M., Design, simulation and bifurcation analysis of a novel micromachined tunable capacitor with extended tenability, *Transactions of the Canadian Society for Mechanical Engineering*, 38(1), 2014, 15-29.
[10] Zamanzadeh, M., Jafarsadeghi-Pournaki, I., Ouakad, H.M., A resonant pressure MEMS sensor based on levitation force excitation detection, *Nonlinear Dynamics*, 100(2), 2020, 1105-1123.
[11] Moory-Shirbani, M., Sedighi, H.M., Ouakad, H.M., Najar, F., Experimental and mathematical analysis of a piezoelectrically actuated multilayered imperfect microbeam subjected to applied electric potential, *Composite Structures*, 184, 2018, 950-960.
[12] Yahiaoui, R., Zeggari, R., Malapert, J., Manceau, J-F., A MEMS-based pneumatic micro-conveyor for planar micromanipulation, *Mechatronics*, 22(5), 2012, 515-521.
[13] Atabak, R., Sedighi, H.M., Reza, A., Mirshekari, E., Instability analysis of bi-axial micro-scanner under electromagnetic actuation including small scale and damping effects, *Microsystem Technologies*, 26, 2020, 1-24.
[14] Siahpour, S., Zand, M.M., Mousavi, M., Dynamics and vibrations of particle-sensing MEMS considering thermal and electrostatic actuation, *Microsystem Technologies*, 24(3), 2018, 1545-1552.
[15] Zhang, W.M., Yan, H., Peng, Z.K., Meng, G., Electrostatic pull-in instability in MEMS/NEMS: A review, *Sensors and Actuators A: Physical*, 214, 2014, 187-218.
[16] Ouakad, H.M., Comprehensive numerical modeling of the nonlinear structural behavior of MEMS/NEMS electrostatic actuators under the effect of the van der Waals forces, *Microsystem Technologies*, 23(12), 2017, 5903-5910.
[17] Azizi, A., Mobki, H., Rezazadeh, G., Bifurcation behavior of a capacitive micro-beam suspended between two conductive plates, *International Journal of Sensor Networks and Data Communications*, 5(149), 2016, 1-10.
[18] Do, C., Lishchynska, M., Delaney, K., Hill, M., Generalized closed-form models for pull-in analysis of micro cantilever beams subjected to partial electrostatic load, *Sensors and Actuators A: Physical*, 185, 2012, 109-116.
[19] Kaveh Rashvand, K., Rezazadeh, G., Mobki, H., Ghayesh, M.H., On the size-dependent behavior of a capacitive circular micro-plate considering the variable length-scale parameter, *International Journal of Mechanical Sciences*, 77, 2013, 333-342.
[20] Fard, K.M., Gharechahi, A., Fard, N.M., Mobki, H., Investigation of dynamic instability of three plates switch under step DC voltage actuation using modified couple stress theory, *Latin American Journal of Solids and Structures*, 15(7), 2018, 1-17.
[21] Wang, B., Zhou, S., Zhao, J., Chen, X., Size-dependent pull-in instability of electrostatically actuated microbeam-based MEMS, *Journal of Micromechanics and microengineering*, 21(2), 2011, 027001.
[22] Kamon, M., Maity, S., Reus, D.D., Zhang, Z., Cunningham, S., Kim, S., Killop, J.M., Morris, A., Lorenz, G., Daniel, L., New simulation and experimental methodology for analyzing pull-in and release in MEMS switches, *Transducers & Eurosensors XXVII: The 17th International Conference on Solid-State Sensors, Actuators and Microsystems (TRANSDUCERS & EUROSENSORS XXVII)*, Barcelona, 2013.
[23] Somà, A., Saleem, M.M., Margesin, B., Armando, M., Pull-in tests of MEMS specimens for characterization of elastic–plastic behavior, *Microsystem Technologies*, 25(7), 2019, 2525-2533.
[24] Pallay, M., Towfighian, S., A reliable MEMS switch using electrostatic levitation, *Applied Physics Letters*, 113(21), 2018, 213102.
[25] Han, J., Li, L., Jin, G., Ma, W., Feng, J., Jia, H., Chang, D., Qualitative identification of the static pull-In and fundamental frequency of one-electrode MEMS resonators, *Micromachines*, 9(12), 2018, 614.
[26] Tahani, M., Askari, A.R., Accurate electrostatic and van der Waals pull-in prediction for fully clamped nano/micro-beams using linear universal graphs of pull-in instability, *Physica E: Low-dimensional Systems and Nanostructures*, 63, 2014, 151-159.
[27] Raman, R., Shanmuganantham, T., Sindhanaiselvi, D., Analysis of RF MEMS series switch with serpentine spring shaped cantilever beam for wireless applications, *Materials Today: Proceedings*, 5(1), 2018, 1890-1896.
[28] Zulkefli, M.A., Mohamed, M.A., Siow, K.S., Majlis, B.Y., Kulothungan, J., Muruganathan, M., Mizuta, H., Three-dimensional finite element method simulation of perforated graphene nano-electro-mechanical (NEM) switches, *Micromachines*, 8(8), 2017, 236.
[29] Najmi, M., Wahid, M.H.A., Johari, S., Mahayudin, A.F.A., Zainol, Z., MEMS parallel plate beam actuator: Correlation study of pull-in voltage and dielectric layer beyond 1µm displacement, *International Electronic Conference on Sensors and Applications session MEMS and NEMS*, MDPI, 2014.

[30] Mobki, H., Sadeghi, M.H., Afrang, S., Rezazadeh, G., On the tunability of a MEMS based variable capacitor with a novel structure, *Microsystem Technologies*, 17(9), 2011, 1447-1452.
[31] Afrang, S., Mobki, H., Hassanzadeh, M., Rezazadeh, G., Design and simulation of a MEMS analog micro-mirror with improved rotation angle, *Microsystem Technologies*, 25(3), 2019, 1099-1109.
[32] Apuzzo, A., Barretta, R., Fabbrocino, F., Faghidian, S.A., Luciano, R., Sciarra, F.M., Axial and torsional free vibrations of elastic nano-beams by stress-driven two-phase elasticity, *Journal of Applied and Computational Mechanics*, 5(2), 2019, 402-413.
[33] Abbondanza, D., Battista, D., Morabito, F., Pallante, C., Barretta, R., Luciano, R., Sciarra, F.M., Ruta, G., Linear dynamic response of nanobeams accounting for higher gradient effects, *Journal of Applied and Computational Mechanics*, 2(2), 2016, 54-64.
[34] Barretta, R., Faghidian, S.A., Sciarra, F.M.D., Stress-driven nonlocal integral elasticity for axisymmetric nano-plates, *International Journal of Engineering Science*, 136, 2019, 38-52.
[35] Romano, G., Barretta, R., Nonlocal elasticity in nanobeams: the stress-driven integral model, *International Journal of Engineering Science*, 115, 2017, 14-27.
[36] Barretta, R., Canadija, M., Luciano, R., Sciarra, F.M., Stress-driven modeling of nonlocal thermoelastic behavior of nanobeams, *International Journal of Engineering Science*, 126, 2018, 53-67.
[37] Beni, Z.T., Ravandi, S.H., Beni, Y.T, Size-dependent nonlinear forced vibration analysis of viscoelastic/piezoelectric nano-beam, *Journal of Applied and Computational Mechanics*, 7(4), 2021, 1878-1891.
[38] Eltaher, M.A., Agwa, M., Kabeel, A., Vibration analysis of material size-dependent CNTs using energy equivalent model, *Journal of Applied and Computational Mechanics*, 4(2), 2018, 75-86.
[39] Ghodrati, B., Yaghootian, A., Zadeh, A.G., Mohammad-Sedighi, H., Lamb wave extraction of dispersion curves in micro/nano-plates using couple stress theories, *Waves in Random and Complex Media*, 28(1), 2018, 15-34.
[40] Keivani, M., Koochi, A., Kanani, A., Mardaneh, M.R., Sedighi, H.M., Abadyan, M., Using strain gradient elasticity in conjunction with Gurtin–Murdoch theory for modeling the coupled effects of surface and size phenomena on the instability of narrow nano-switch, *Proceedings of the Institution of Mechanical Engineers, Part C: Journal of Mechanical Engineering Science*, 231(17), 2017, 3277-3288.
[41] Soltani, D., Khorshidi, M.A., Sedighi, H.M., Higher order and scale-dependent micro-inertia effect on the longitudinal dispersion based on the modified couple stress theory, *Journal of Computational Design and Engineering*, 8(1), 2021, 189-194.
[42] Abdehvand, M.Z., Roknizadeh, S.A.S., Sedighi, H.M., Modeling and analysis of a coupled novel nonlinear magneto-electro-aeroelastic lumped model for a flutter based energy harvesting system, *Physica Scripta*, 96(2), 2020, 025213.
[43] Mobki, H., Rezazadeh, G., Sadeghi, M., Vakili-Tahamia, F., Seyyed-Fakhrabadi, M-M., A comprehensive study of stability in an electro-statically actuated micro-beam, *International Journal of Non-Linear Mechanics*, 48, 2013, 78-85.
[44] Rao, S.S., *Vibration of Continuous Systems*, John Wiely & Sons, New Jersy, 2007.
[45] Vakili-Tahami, F., Mobki, H., Keyvani-Janbahan, A-A., Rezazadeh, G., Pull-in phenomena and dynamic response of a capacitive nano-beam switch, *Sensors & Transducers*, 110(11), 2009, 26-37.
[46] Hagan, M.T., Demuth, H.B., Beale, M., *Neural network design*, PWS Publishing Co, USA, 1997.
[47] Azimloo, H., Rezazadeh, G., Shabani, R., Sheikhlou, M., Bifurcation analysis of an electro-statically actuated micro-beam in the presence of centrifugal forces, *International Journal of Non-Linear Mechanics*, 67, 2014, 7-15.
[48] Rokni, H., Seethaler, R.J., Milani, A.S., Hosseini-Hashemi, S., Li, X.F., Analytical closed-form solutions for size-dependent static pull-in behavior in electrostatic micro-actuators via Fredholm integral equation, *Sensors and Actuators A: Physical*, 190, 2013, 32-43.
[49] Haluzan, D.T., Klymyshyn, D.M., Achenbach, S., Börner, M., Reducing pull-in voltage by adjusting gap shape in electrostatically actuated cantilever and fixed-fixed beams, *Micromachines*, 1(2), 2010, 68-81.
[50] Sadeghian, H., Rezazadeh, G., Osterberg, P.M., Application of the generalized differential quadrature method to the study of pull-in phenomena of MEMS switches, *Journal of Microelectromechanical Systems*, 16(6), 2007, 1334-1340.
[51] Rezazadeh, G., Tahmasebi, A., Zubstov, M., Application of piezoelectric layers in electrostatic MEM actuators: controlling of pull-in voltage, *Microsystem Technologies*, 12(12), 2006, 1163-1170.

ORCID iD

Mortaza Aliasghary https://orcid.org/0000-0002-2638-8643
Hamed Mobki https://orcid.org/0000-0001-7689-3544
Hassen M. Ouakad https://orcid.org/0000-0001-7262-2130

How to cite this article: Aliasghary M., Mobki H., Ouakad H.M. Pull-in Phenomenon in the Electrostatically Micro-switch Suspended between Two Conductive Plates using the Artificial Neural Network, *J. Appl. Comput. Mech.*, 8(4), 2022, 1222–1235. https://doi.org/10.22055/JACM.2021.38569.3248